Bangladesh J. Bot. **52**(2): 529-538, 2023 (June) Special DOI: https://doi.org/10.3329/bjb.v52i20.68217

DEVELOPMENT AND TEST OF RICE NITROGEN NUTRITION INDEX ESTIMATION MODEL BASED ON AIRBORNE MULTI-SPECTRUM

LIJUAN SONG[1,2*], WANJUN YE[1], SHU WANG[3], SHUBING LIU[1], MEIXUAN WANG[1], GE SU[1] AND HONGWEN BI[1]

Heilongjiang Academy of Agricultural Sciences Postdoctoral Programme, Harbin150086, China

Keywords: Cold-terra rice, Airborne multispectrum, Nitrogen nutrition diagnosis

Abstract

Both excessive and deficient nitrogen (N) concentration in the growing media can affect the growth, development, yield, and quality of rice. Traditional methods of N determination of plant require destructive and rigorous sampling, which is also time-consuming and laborious. However, rapid and non-destructive nitrogen diagnosis has become an important area of research in precision agriculture. Heilongjiang Province, China is a cold climate rice growing area, where the growth and fertilization of rice follows a definite pattern. In the present study, two varieties of rice (Wuyoudao4 and Songjing9) and as location Heilongjiang Province were selected. Nitrogen diagnosis of rice was carried out based on airborne multi-spectrum methodology. Canopy spectral data of rice at key growth periods were obtained by using a UAV equipped with a multi-spectral camera, and agronomic parameters such as leaf N content and dry matter weight were obtained synchronically. An airborne multispectral canopy normalized vegetation index (NDVI) model for N diagnosis based on its critical concentration curve was established as a nondestructive N diagnosis of rice for cold region. Results showed that canopy NDVI can estimate rice nitrogen nutrition index (NNI) properly over the growth period. The coefficient of determination R^2, root mean square error (RMSE) and standard root mean square error (nRMSE) were compared to determine the best effect of the index model. The interphase nitrogen diagnosis model of WYD-4 based on NDVI for cold region was as follows: $NNI=0.3916e^{1.0809*NDVI}$ (RMSE=0.12, nRMSE=12.43%), SJ-9: $NNI=0.3325e^{1.2705*NDVI}$ (RMSE=0.10, nRMSE =10.36%), indicating that the established model can better estimate the nitrogen status of rice.

Introduction

In analyzing the nutritional status of plants, spectral remote sensing technology is used via detecting the optical reflection of the leaves or the spectral characteristics of the leaves and canopy. Compared with the traditional methods of crop nutrition diagnosis, spectral remote sensing technology has an advantage to cover large cropping areas with no damage to the crop and with minimum time. Thus, the technology can play an important role in guiding N fertilizer application in precision agriculture. Nitrogen deficiency or its excessive concentration in crops causes changes in plant leaf color, thickness, moisture content, and morphological structure, which can lead to changes in canopy spectral characteristics. All these are considered as the theoretical basis for spectral remote sensing technology to diagnose crop N status. Literature available in favor of use of spectral remote sensing technology in corn (Tumbo *et al.* 2002, Miao *et al.* 2009), rice (Xue *et al.* 2003), barley (Tang *et al.* 2003), wheat (Jia *et al.* 2004, Liu, *et al.* 2004), and beans (Maderia *et al.* 2000). A correlation between leaf chlorophyll content and its spectral characteristics was found. Tumbo *et al.* (2002) reported chorophyll as the main factor causing the difference in spectral characteristics. Xue *et al.* (2003) observed that spectral reflectance of rice canopy was significantly correlated with leaf N content. Therefore, it appears that spectral characteristics can be used to monitor N status of plants.

*Author for correspondence: <songlijuan-2007@163.com>. [1]Heilongjiang Academy of Agricultural Sciences, Harbin150086, China [2]Heilongjiang University of Science and Technology, Harbin 150022, China. [3]College of Agronomy, Shenyang Agricultural University, Shenyang110866, China.

Satellite remote sensing technology can be easily interfered by weather and geographical environment, and therefore image data acquisition comes difficult with high operational cost. On the other hand, ground remote sensing operations are unable to cover a large area because it is time-consuming, labor intensive, and low operation efficiency. Therefore, remote sensing of UAV emerges as the complementary to solve those problems. The technology is fast, efficient, low cost and simple operation. Thus, UAV fertilization decision-making (Pei *et al.* 2018, Tian *et al.* 2018, Sun *et al.* 2019, Wang *et al.* 2018, Wu *et al.* 2019, Zang *et al.* 2019) specially in the small and medium-sized family farms, cooperatives and other areas has good prospects for development and use. Most of the previous studies used canopy spectral index, plant and leaf N content, leaf SPAD value and other indicators to develop N nutrient diagnostic models, and most of the established models were diagnostic models of a single period (Yang *et al.* 2019, Xu *et al.* 2023). There are few studies on N nutrition diagnosis based on NDVI and NNI in the cold region of Northeast China. Therefore, in the present study, NDVI was used to estimate the nitrogen status of rice in the cold region during the key growth period, so as to provide necessary data support for N nutrition diagnosis and growth analysis of crops. Meanwhile, the validity of multi-spectral remote sensing data obtained by UAV was verified, which provided more theoretical basis for rational application of N in japonica rice in the cold region.

Materials and Methods

In the present investigation, two (2) divided experiments were carried out from 2016-17. All the basic information related to the experiment is presented in Table 1.

Table 1. Basic information of two experiments.

Experiment no.	(Transplanting/ harvesting date)	Location	Cultivar	N rate (kg/ha)	Sampling stage	Soil characteristics
Experiment 1 in 2016	20-May/ 25-Sep	Wuchang (44°92′N, 127°15′E)	Wuyoudao4 Songjing9	N_0(0) N_{60}(60) N_{120}(120) N_{180}(180) N_{240}(240)	Active tillering Panicle initiation Stem elongation Booting Heading Grain filling	Soil type = Brunisolic Soil pH= 6.59 Total P = 2.15 g/kg Total K = 17. 5g/kg Available N = 114 ppm Available P = 37.8 ppm Available K = 156 ppm
Experiment 2 in 2017	18-May/ 24-Sep	Wuchang (44°92′N, 127°15′E)	Wuyoudao4 Songjing9	N_0(0) N_{60}(60) N_{120}(120) N_{180}(180) N_{240}(240)	Active tillering Panicle initiation Stem elongation Booting Heading Grain filling	Same as above

Two cultivars of rice (*Oryza sativa* L.) *viz.* Wuyoudao4 and Songjing9 were use in this experiment. Data on crop growth from five separate hills were collected during active tillering to heading stages (before onset of flowering) at an interval of 10-12 d, starting from 16 and 18 d after transplanting (DAT) in 2016 and 2017, respectively. After completion of field data acquisition, the whole plants were manually uprooted and samples were divided into leaf blades (leaf) and culms plus sheaths (stem), and fresh plants were separated into different leaves i.e. green parts and rest of the leaf parts, other than green leaves. These samples were analyzed for determining biomass, N content, and yield.

Shoot biomass (t/ha) was determined by cutting five plants from each plot at ground level on each sampling date. Fresh plants were separated into leaf blades (leaves) and culms plus sheaths (stems). Leaf dry matter (LDM) was determined after each sample was oven-dried at 80◦C for 48 hrs. At maturity, the total number of panicles in each plot was investigated. At the same time, 30 plants were selected for indoor seed examination. Grain number per panicles, grain weight per panicles, and 1000-grain weight were recorded. The leaf samples were subsequently ground to a powder form to pass through a 1-mm sieve in a Wiley Mill and stored at room temperature until further chemical analysis. Total N concentration of leaf samples was determined by using the micro-Kjeldahl method (Lu *et al.* 2015).

SPAD values were measured from 10 randomly selected plants from each field plot with the help of a SPAD-502 meter (Minolta Camera Co., Osaka, Japan). The measurement was carried out from the four uppermost fully expanded leaves, designated asL1, L2, L3, and L4, respectively. Ten randomly selected plants from each field plot were measured SPAD that the leaf of around the midpoint as the mean SPAD value (Jia *et al.* 2004).

During crop growth period, spectral data of rice canopy at tillering, stem elongation, booting, heading, grain filling, and other key growth stages were collected. For the purpose, a four-axis eight-rotor UAV (EWT-S1) equipped with mini-MCA 6 and Incident Light Sensor multi-spectral array camera produced by Tetracam was used. The multi-spectral camera has six spectral acquisition channels, including blue (470 nm), green (550 nm), red (690 nm), orange-red (660 nm), red-edge (710 nm), and near-infrared (810 nm) bands. Each channel uses a 25 mm diameter filter with a focal length of 9.6 mm. Images are stored in RAW format. During operation, the UAV flies at a height of 100 m with the safe cruising speed ~15 m/s having ground resolution 0.05 m. The ground is covered with calibration blankets with different reflectance of black, white, and gray. The laying position should ensure that the images taken are in the same image, instead of using the whiteboard to verify before and after data collection. From 10:00 - 14:00 h, a cloudless day was selected to collect canopy spectral data. During the flight, EWT-S1 UAV ground station was used to obtain the location and altitude of camera points. The use of mini-MCA 6 multi-spectral camera image processing software PiexlWrench 2 to pre-process the multi-spectral image to complete atmospheric correction and radiation calibration, because of the modification of the UAV remote control system, in the multi-spectral camera and remote-control system to increase a weak current single-chip microcomputer closing system. The remote control of the shutter of the multi-spectral camera is realized, and the area required for shooting was coordinated with the ground receiving system, so the image completely covers the whole test cell, and no image stitching is required. The image processing software PiexlWrench 2 selected the test area and extracted the canopy NDVI value.

The linear relationships and 95% confidence limits were calculated using SPSS 22 (SPSS Inc., Chicago, IL, USA) with different SPAD and N indicators at five growth stages, including tillering (TI), panicle initiation (PI), stem elongation (SE), booting (BT), and heading (HD), using the values collected in the experiment (Table1). Among the five growth stages, the key N management stages are SE, PI, and BT. Therefore, the indicators to build up the models with an exponential function not only for these specific growth stages, but also for the entire the growth period of crop was selected. The SPAD indicators for the different leaf positions were calculated as shown in Table 2 (Yuan *et al.* 2016).

For the N indicators, LNC was used to represent the green leaf N concentration based on the leaf dry matter in the formula below:

$$NNI=Na/Nc \quad (1)$$

where Na is the actual LNC and Nc is the critical nitrogen of japonica rice based on leaf dry matter previously determined by Song *et al.* (2020)

$$\text{Wuyoudao4}: Nc=1.96LDM^{-0.56} \quad (2)$$

$$\text{Songjing9}: Nc=1.99LDM^{-0.44} \quad (3)$$

Table 2. SPAD values in different leaf positions of rice canopy and method for calculating the normalized SPAD values.

SPAD indicator	Formula	Note
L1	The SPAD values from the top sides of the first fully expanded leaves of rice	
L2	The SPAD values from the top sides of the second fully expanded leaves of rice	
L3	The SPAD values from the top sides of the third fully expanded leaves of rice	
L4	The SPAD values from the top sides of the fourth fully expanded leaves of rice	
NSI1	NSI1=L1(i)/L1 in the treatment with the highest N rate	L1(i) instead the SPAD values from the top sides of the first fully expanded leaves of rice
NSI2	NSI2=L2(i)/L2 in the treatment with the highest N rate	L2(i) instead the SPAD values from the top sides of the second fully expanded leaves of rice
NSI3	NSI3=L3(i)/L3 in the treatment with the highest N rate	L3(i) instead the SPAD values from the top sides of the third fully expanded leaves of rice
NSI4	NSI4=L4(i)/L4 in the treatment with the highest N rate	L4(i) instead the SPAD values from the top sides of the fourth fully expanded leaves of rice
DSI	DSI=L1-L3	
RSI	RSI=L1/L3	
RDSI	RDSI=(L1-L3)/L3	
NDSI	NDSI=(L1-L3)/(L1+L3)	

Microsoft Excel 2016 and SPSS 22.0 statistical analysis software were used for data calculation and statistical analysis. GraphPad Prism 7.0 mapping software was used for plotting. Based on the experimental data of 2017, the correlation analysis of the NDVI, LNC, NNI, L4, and NSI4 in the cold region was conducted. The spectral model of rice N nutrient index in cold region was determined by regression fitting method. Independent test data in 2016 were used to verify the model. Internationally common RMSE, nRMSE, and R^2 were used to evaluate the constructed model (Yang *et al.* 2000, Jamieson *et al.* 1991).

Results and Discussion

As shown in Fig.1, the NDVI of two rice varieties firstly increased and then decreased during the whole growth period. With the increase of nitrogen application level, NDVI increased but the increase of canopy NDVI gradually slowed down. At the early growth stage, NDVI was affected by bare ground and water layer, and NDVI was relatively low. Therefore, the regression analysis of canopy NDVI and N nutrient index (leaf nitrogen content and nitrogen nutrient index) and canopy leaf SPAD index were carried out at stem elongation booting and heading stages, respectively.

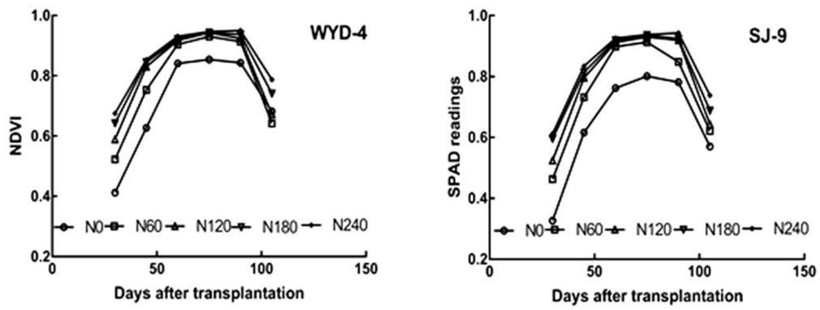

Fig. 1. Changes of canopy NDVI of two rice cultivars at different N application levels under and different growth stages

The results of variance analysis of N nutrition status of rice in cold regions with different nitrogen application levels (Table 3). In 2017, under 5 fertilization levels, the LNC, NNI, L4, NSI4, and other data of different rice varieties were analyzed. Under the experimental conditions of the present study, from stem elongation stage to heading stage, the N nutrition status of rice canopy in cold area was mainly affected by N fertilization level, and there were significant differences among the N application levels ($P<0.01$).

Table 3. Analysis of variance for N concentration of leaves at different fertilizer N levels.

Indicator	Variation source	Sum of Squares	df	Mean square	F-value	P-value
	Between Groups	4.958	4	1.240	9.205	0.000
LNC	Within Groups	11.446	85	0.135		
	Total	16.404	89			
	Between Groups	2.136	4	0.534	227.181	0.000
NNI	Within Groups	0.200	85	0.002		
	Total	2.335	89			
	Between Groups	2251.713	4	562.928	122.833	0.000
L4	Within Groups	389.546	85	4.583		
	Total	2641.259	89			
	Between Groups	0.996	4	0.249	139.090	0.000
NSI4	Within Groups	0.152	85	0.002		
	Total	1.148	89			

Results of analysis of variance (ANOVA) of N nutrition status of rice at different growth stages in cold region are shown in Table 4. There were no significant differences among NNI, L4, and NSI4 at different growth stages ($P > 0.05$), while the difference in leaf nitrogen content at the stem elongation stage, booting stage, and heading stage is extremely significant ($P < 0.01$).

Table 4. Analysis of variance of N concentration of plants at different growth stages.

Indicator	Variation source	Sum of Squares	df	Mean square	F-value	P-value
LNC	Between Groups	10.941	2	5.470	87.112	0.000
	Within Groups	5.463	87	0.063		
	Total	16.404	89			
NNI	Between Groups	0.057	2	0.028	1.082	0.344
	Within Groups	2.279	87	0.026		
	Total	2.335	89			
L4	Between Groups	44.086	2	22.043	0.738	0.481
	Within Groups	2597.173	87	29.853		
	Total	2641.259	89			
NSI4	Between Groups	0.014	2	0.007	0.556	0.576
	Within Groups	1.134	87	0.013		
	Total	1.148	89			

In the present study, N nutrition indexes mainly included leaf N content, nitrogen nutrition index, and SPAD value and normalized SPAD index of the fourth fully developed leaf. As it can be seen from Table 5, there was a significant positive correlation between canopy NDVI and N nutrition index of the two rice varieties at different growth stages i.e., extremely significant positive correlation at the stem elongation stage and significant correlation between booting stage and heading stages. The linear determination coefficients R^2 of leaf N content and N nutrient index of WYD-4 rice and canopy NDVI at different growth stages ranged from 0.518 - 0.911 and 0.521 - 0.941, respectively. The linear determination coefficients R^2 of leaf N content and N nutrient index of SJ-9 rice and canopy NDVI at different growth stages ranged from 0.577 - 0.738 and 0.531 - 0.767, respectively. The linear determination coefficients R^2 of canopy NDVI, L4 and NSI4 ranged from 0.574 - 0.814 and 0.548 - 0.817, respectively. Canopy NDVI of SJ-9 rice variety and the linear determination coefficients R^2 of L4 and NSI4 ranged from 0.521 - 0.782 and 0.519 - 0.762, respectively. On the whole, the linear correlation coefficient R2 of WYD-4 rice variety was higher than that of SJ-9 rice variety.

The linear determination coefficients R^2 of nitrogen nutrition indices (LNC, NNI, L4, NSI4) and canopy NDVI were the highest in both cultivars at the stem elongation stage ($p<0.01$). With the development of growth process, the linear determination coefficient R^2 of nitrogen nutrition index and canopy NDVI decreased successively. It might be due to the fact that after the booting stage, the rice headed and flowering successively, and the canopy spectral determination changed, which led to the change of canopy NDVI. NNI is an effective means for N nutrition diagnosis. Since NNI in variance analysis is not significantly affected by growth period, data of the three growth periods are summarized and analyzed, and the results are shown in Table 6. In summary of the three growth periods, there was a significant correlation between canopy NDVI and NNI of the two varieties. The linear determination coefficient R^2 of SJ-9 was 0.479 ($p<0.01$), and that of WYD-4 was 0.360 ($p<0.05$). Further, regression modeling analysis would be conducted.

Table 6 summarizes the modeling determination coefficient R^2, validation determination coefficient R^2, root mean square error RMSE and standard root mean square error nRMSE of five models from the index, comparative linearity, logarithm, quadratic term and power function between canopy NDVI and NNI of two rice varieties at the stem elongation-heading stage. The coefficient of determination of WYD-4 index model was the highest, with R^2 of 0.376 ($p<0.01$), and the coefficient of determination of SJ-9 quadratic model was the highest, with R^2 of 0.505 ($p<0.01$). However, considering the evaluation indexes such as model validation coefficient R^2, root mean

Table 5. Linear coefficients of canopy NDVI and Nitrogen Index of different rice cultivar at different growth periods.

Cultivar	Indicator	Determination coefficient (R^2)		
		SE	BT	HD
WYD-4	LNC	0.911^{**}	0.518^{*}	0.609^{*}
	NNI	0.941^{**}	0.521^{*}	0.626^{*}
	L4	0.814^{**}	0.651^{**}	0.574^{*}
	NSI4	0.817^{**}	0.586^{*}	0.548^{*}
SJ-9	LNC	0.738^{**}	0.637^{*}	0.577^{*}
	NNI	0.767^{**}	0.531^{*}	0.583^{*}
	L4	0.782^{**}	0.619^{*}	0.521^{*}
	NSI4	0.762^{**}	0.619^{*}	0.519^{*}

**significance at 0.01; * significance at 0.05; n=15, $r_{0.01}=0.641$, $r_{0.05}=0.514$.

square error RMSE and standard root mean square error nRMSE, the results showed that the model modeling effect of the two varieties was better. Although the coefficient R^2 of the interphase (stem elongation-heading stage) model was lower than that of the single period model, both reached the extremely significant level of 0.01. The model of stem elongation and booting period was:

WYD-4: $NNI=0.3916e^{1.0809*NDVI}$, $R^2=0.376(P<0.01)$ (4)

SJ-9: $NNI=0.3325e^{1.2705*NDVI}$, $R^2=0.502(P<0.01)$ (5)

In the present study, independent test data in 2016 were used to verify the nitrogen diagnosis interval model established by canopy NDVI and NNI during stem elongation and booting stages. As shown in Fig. 2, rice varieties R^2, RMSE and nRMSE of WYD-4 were 0.335, 0.12 and 12.43%, respectively. SJ-9 rice varieties R^2, RMSE and nRMSE were 0.666, 0.10 and 10.36% respectively. The relationship between the observed and simulated values of NNI was good. The model accuracy evaluation value RMSE of the two varieties was small, and the model stability evaluation value nRMSE was basically within 20%. The model performance was stable and reached a good level, indicating that the model developed based on canopy NDVI and NNI had higher prediction accuracy and better stability. It can be used for N nutrition diagnosis of rice in the cold region.

In a study of winter wheat, Hu *et al.* (2010) found that the linear correlation between leaf nitrogen and chlorophyll content and canopy NDVI at jointing stage and milk ripening stage was consistent with SPAD value, and nitrogen diagnosis could be carried out at jointing stage of winter wheat. Results of this study showed that the canopy normalized vegetation index NDVI at the early tillering stage was low, because the rice field was not covered by plant canipy. At the early growth stage, and soil background and water layer had certain influence on the spectral measurement. Therefore, the canopy normalized vegetation index NDVI at the early growth stage of rice was not suitable for nitrogen nutrition diagnosis due to the influence of soil background. This is consistent with the results of rice nitrogen estimation by Chen *et al.* (2014). Although, the correlation coefficient of nitrogen estimation using Greenseeker is high, RMSE and nRMSE are also high, and the accuracy and stability of the model are poor. Therefore, the measurement should be carried out after the rice fields are closed in the monitoring process to reduce the estimation error, improving the estimation accuracy and the stability of the model.

Table 6. NDVI and NNI regression analysis model for rice cultivars.

Cultivar	Types	Model building	Model validation		
		R^2	R^2	RMSE	NRMSE (%)
WYD-4	E	0.376^{**}	0.335^{*}	0.12	12.43
	Log	0.351^{*}	0.322^{*}	0.13	12.61
	Q	0.366^{*}	0.339^{*}	0.12	12.45
	P	0.368^{*}	0.329^{*}	0.12	12.49
	L	0.360^{*}	0.330^{*}	0.12	12.54
SJ-9	E	0.502^{**}	0.666^{**}	0.10	10.36
	Log	0.463^{**}	0.659^{**}	0.10	10.85
	Q	0.505^{**}	0.644^{**}	0.10	11.01
	P	0.489^{**}	0.664^{**}	0.10	10.38
	L	0.479^{**}	0.664^{**}	0.10	10.79

**significance at 0.01; *significance at 0.05; n=45, $r_{0.01}$=0.372, $r_{0.05}$=0.288.

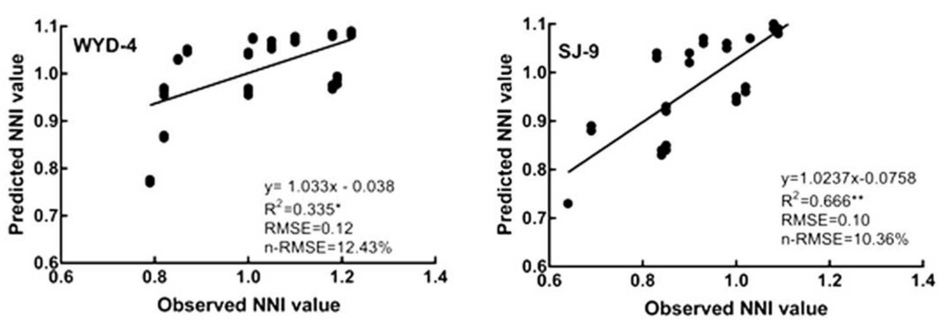

Fig. 2. Correlation between observed and predicted values of NNI for two rice cultivars.

NDVI is an important index reflecting vegetation coverage, which can eliminate most of the irradiance changes related to instrument calibration, solar angle, terrain, cloud shadow and atmospheric conditions, and enhance the response ability of vegetation index. It is the most widely used vegetation index among the existing ones. NDVI is closely related to crop nitrogen status. Many researchers use normalized vegetation index NDVI to estimate various indexes in different crops (Lu *et al.* 2008, Chen *et al.* 2014, Raun *et al.* 2002), therefore, using NDVI to diagnose nitrogen nutrition is more consistent with the law of biology. In the present study, based on the leaf dry matter critical nitrogen concentration dilution curve model, canopy NDVI was obtained by using UAV and multi-spectral camera, and canopy NDVI and NNI estimation models were developed to estimate the NNI value of japonica rice under different N application levels, and the basic theory of N nutrient index was applied to guide the precise fertilization in the field. Because canopy NDVI is easily affected by field radiation, soil background, water layer and other factors, the established model is extremely significant at the level of 0.01, but the coefficient of determination is relatively low. In the future, the above factors should be taken into account and new modeling methods should be explored to improve the test results.

The multi-spectral camera used in this study can obtain 6 bands, covering the red edge band reflecting crop N status. Compared with the spectral camera with hundreds of bands, the effective band spectral information is retained, and the workload of lengthy information and data processing is reduced. Using the software of the camera to extract NDVI is simple and convenient for application and practical operation. However, agricultural low altitude remote sensing technology is still a complex system engineering. China is still in the primary stage in this field, and further research is still needed in the future.

Results of variance analysis showed that the monitoring of rice NNI in the cold region was less affected by the growth period. By comparing the determination coefficients R2, RMSE, nRMSE and so on, the index model has the best effect in estimating NNI with normalized vegetation index NDVI.WYD-4: $NNI=0.3916e^{1.0809*NDVI}$, $R^2=0.376(P<0.01)$, RMSE=0.12, nRMSE =12.43%; SJ-9: $NNI=0.3325e^{1.2705*NDVI}$, $R^2=0.502(P<0.01)$, RMSE=0.10, nRMSE=10.36%.

The UAV platform equipped with multi-spectral camera has good feasibility to dynamically monitor the nitrogen status of rice canopy in the cold region, which can solve the problems of time-consuming and laborious and limitations of destructive sampling. It is a good choice for small and medium-sized regional scale applications.

Acknowledgments

This research was funded by the research institute research expenses project of Heilongjiang (CZKYF2021-2-B010); Postdoctoral project of Heilongjiang (LBH-Z21078); Economic and social development key research topic of Heilongjiang (22243); Heilongjiang Academy of Agricultural Sciences (2021JCQN005, HNK2019CX12-16,2019YYYF022).

References

Chen QC, Tian YC, Xia Y, Cao WX and Zhu Y 2014. Comparison of five nitrogen dressing methods to optimize rice growth. Plant Prod. Sci, **17**(1): 66-80.

Jamieson PD, Porter JR and Wilson DR 1991. A test of the computer simulation model ARCWHEAT1 on wheat crops grown in New Zealand. Field Crop. Res. **27**: 337-350.

Jia LL, Cheng XP, Zhang F, Buerkert A and Romhelo V 2004. Use of digital camera to assess nitrogen status of winter wheat in the northern China Plain. J. Plant. Nutr. Soil Sci, **27**(3): 441-450.

Liu HB, Zhang YG, Li ZH, Zhang CY and Hu DY 2004. Application of canopy spectral reflectance in monitoring nitrogen status of winter wheat. Sci. Agricul. Sin. **37**(11): 1743-1748.

Hu H, Bai YL, Yang LP, Lu YL, Wang L, Wang H and Wang ZY 2010. Diagnosis of nitrogen nutrition in winter wheat (Triticum aestivum) via SPAD-502 and GreenSeeker. Chin. J. Eco-Agricul. 18(4):748-752.

Lu ZZ 2015. Study on critical nitrogen concentration and spectral index model of rice in the lower reaches of the Yangtze River. Ph.D. Thesis, Nanjing Agricultural University, Nanjing, China.

Maderia AC, Mentions A, Ferreira ME and Maria de LT 2000. Relationship between spectroradiometric and chlorophyll measurements in green beans. Commun Soil Sci Plant Anal. **31**(6): 631-643.

Miao YX, Mulla DJ, Randall GW, Vetsch JA and Vintila R 2009. Combining chlorophyll meter readings and high spatial resolution remote sensing images for in-season site-specific nitrogen management of corn. Precis. Agric. **10**: 45-62.

Pei XB, Wu HL, Ma P, Yan YF, Peng C, Hao L and Bai Y 2018. Analysis of the spectrum and vegetation index of rice under different nitrogen levels based on unmanned aerial vehicle remote sensing. Chinese Optics, **11**(5): 832-840.

Raun WR, Solie JB, Johnson GV, Stone ML, Mullen RW, Freeman KW, Thomason WE and Lukina EV 2002. Improving nitrogen use efficiency in cereal rain production with optical sensing and variable rate application. Agron J. **94**(4): 815-820.

Sun MM, Shen JH and Ren SP 2019.Evaluation of control effect of UAV spray on rice pests by adding adjuvant. Hunan Agricul. Sci. **9**: 55-57.

Song LJ, Wang S and Ye WJ 2020. Establishment and application of critical nitrogen dilution curve for rice based on leaf dry matter. Agron. 10, 367; doi:10.3390/agronomy10030367.

Tumbo SD, Wagner DG and Heinemann PH 2002. Hyper spectral characteristics of corn plants under different chlorophyll levels. Trans. ASABE. **45**(3): 815-823.

Tang YL, Wang RC, Zhang JH and Wang K 2003. Study on determining nitrogenous levels of barley by hyperspectral and chlorophyll meter. J. Triticeae Crops. **23**(1): 63-66.

Tian ML, Ban ST, Yuan T, Ji YB, MA C and Li LY 2018. Monitoring of lodged rice using low-altitude UAV based multispectral image. Acta Agricul. Shanghai. **34**(6): 88-93.

Wu FM, Zhang M and Wu BF 2019. Rapid object-oriented rice planting area extraction from UAV images. J. Geoinform. Sci. **21**(5): 789-798.

Wang Z, Chu GK, Zhang HJ, Liu SX, Huang XC, Gao FR, Zhang CQ and Wang JX 2018. Identification of diseased empty rice panicles based on Haar-like feature of UAV optical image. Trans. Chin. Soc. Agricul. Engin. **34**(20): 73-82.

Xue LH, Cao WX, Luo WH, Jiang D, Meng YL and Zhu Y 2003. Diagnosis of nitrogen status in rice leaves with the canopy spectral reflectance. Sci. Agricul. Sin. **36**(7): 807-812.

Xu TY, Bai JC, Guo ZH, Jin ZY, Yu FH 2023. Diagnosis method of rice nitrogen deficiency based on UAV hyperspectral remote sensing. Transactions Chin. Soc. Agricul. Mach. **2**: 189-222.

Yang J, Greenwood DJ, Rowell DL, Wadsworth GA and Burns IG 2000. Statistical methods for evaluating a crop nitrogen simulation model. Agr. Syst. **64**: 37-53.

Yuan ZF, Cao Q, Zhang K, Ata-Ul-Karim, Tian YC, Zhu Y, Cao WX and Liu XJ 2016. Optimal leaf positions for SPAD meter measurement in rice. Front Plant Sci. **7**: 719.

Yang HY, Zhou Q, Yang J, Sun YT, Lu Y and Yin H 2019. Study on nitrogen nutrition diagnosis of rice leaves based on hyperspectrum. Acta Agricul. Zhejiangensis **31**(10): 1575-1582.

Zang Y, Hou XB, Wang P, Zhou ZY, Jiang R and Li KL 2019. A study on Huanghuazhan rice fertilization decision model based on remote sensing technology of unmanned aerial vehicle. J. Shenyang Agricul. University **50**(3): 324-330.

(Manuscript received on 06 March, 2023; revised on 19 May, 2023)